JOURNAL OF BACTERIOLOGY, Feb. 1997, p. 1165–1173 Vol. 179, No. 4
0021-9193/97/$04.00+0

Functional Domains of *Agrobacterium tumefaciens* Single-Stranded DNA-Binding Protein VirE2†

PRISCILLA DOMBEK[1]‡ AND WALT REAM[2,3]*

Department of Biochemistry & Biophysics,[1] Molecular and Cellular Biology Program,[2] and Department of Agricultural Chemistry,[3] Oregon State University, Corvallis, Oregon 97331

Received 14 May 1996/Accepted 2 December 1996

The transferred DNA (T-DNA) portion of the *Agrobacterium tumefaciens* tumor-inducing (Ti) plasmid enters infected plant cells and integrates into plant nuclear DNA. Direct repeats define the T-DNA ends; transfer begins when the VirD2 endonuclease produces a site-specific nick in the right-hand border repeat and attaches to the 5′ end of the nicked strand. Subsequent events liberate the lower strand of the T-DNA from the Ti plasmid, producing single-stranded DNA molecules (T strands) that are covalently linked to VirD2 at their 5′ ends. *A. tumefaciens* appears to transfer T-DNA into plant cells as a T-strand–VirD2 complex. The bacterium also transports VirE2, a cooperative single-stranded DNA-binding protein, into plant cells during infection. Both VirD2 and VirE2 contain nuclear localization signals that may direct these proteins, and bound T strands, into plant nuclei. Here we report the locations of functional regions of VirE2 identified by eight insertions of *Xho*I linker oligonucleotides, and one deletion mutation, throughout *virE2*. We examined the effects of these mutations on virulence, single-stranded DNA (ssDNA) binding, and accumulation of VirE2 in *A. tumefaciens*. Two of the mutations in the C-terminal half of VirE2 eliminated ssDNA binding, whereas two insertions in the N-terminal half altered cooperativity. Four of the mutations, distributed throughout *virE2*, decreased the stability of VirE2 in *A. tumefaciens*. In addition, we isolated a mutation in the central region of VirE2 that decreased tumorigenicity but did not affect ssDNA binding or VirE2 accumulation. This mutation may affect export of VirE2 into plant cells or nuclear localization of VirE2, or it may affect an uncharacterized activity of VirE2.

Agrobacterium tumefaciens causes crown gall tumors on many dicotyledonous plant species when the bacterium infects wounded tissue (18). This bacterium harbors the Ti plasmid, where genes essential for tumorigenesis are located (64, 70). The T-DNA portion of the Ti plasmid enters plant cells and integrates into nuclear DNA (8, 9, 72). Tumorous growth results from expression of three T-DNA genes that encode biosynthetic enzymes for two plant growth hormones, auxin (indole acetic acid) and cytokinin (isopentenyl adenosine) (for reviews, see references 46, 73, and 79).

Virulence (*vir*) genes necessary for T-DNA transmission (transfer and integration) lie elsewhere on the Ti plasmid (22, 56). VirA, a signal receptor/kinase protein located in the bacterial membrane, phosphorylates VirG, a transcriptional activator, in response to phenolic compounds (55) and sugars released by wounded plant cells (for reviews, see references 28 and 73). Phosphorylated VirG protein activates transcription of its own gene and other *vir* operons (73). Export of T-DNA and proteins (VirD2 and VirE2) from *A. tumefaciens* into plant cells depends on membrane-associated proteins encoded by the *virB* operon, which contains 11 genes (for reviews, see references 28 and 79), and the *virD4* gene (10, 40). The VirB proteins are similar in amino acid sequence to pertussis toxin liberation (Ptl) proteins of *Bordetella pertussis*, which mediate export of pertussis toxin (15, 71), and to proteins that mediate conjugal transfer of IncPα plasmid RP4 (Trb proteins) (37) and IncN plasmid pKM101 (Tra proteins) (44). VirD4 is similar to TraG, another protein required for conjugal transfer of RP4 (37). Thus, proteins essential for crown gall tumorigenesis appear to permit export of specific Vir proteins and T-DNA into plant cells by pathways similar to those that operate in other bacteria.

T-DNA transfer requires, in *cis*, the right-hand 25-bp border sequence, while deletions that remove it abolish tumorigenesis (43, 51, 66). The loss of a nearby sequence, designated *overdrive*, reduces tumorigenesis several hundredfold (42); the *virC* operon, which is also necessary for full virulence, encodes a protein (VirC1) that binds *overdrive* (63). T-DNA transfer begins when an endonuclease comprised of VirD1 and VirD2 nicks at a specific site within the right-hand border sequence (67, 76) and attaches to the 5′ end of the nicked strand (20, 25, 29, 68, 77). Displacement, in a 5′-to-3′ direction, of the bottom (nicked) strand of the T-DNA produces linear VirD2-bound single-stranded DNAs (ssDNAs) called T strands (1, 32, 57), which the bacterium appears to export into plant cells (59).

A. tumefaciens also exports VirE2 into plant cells via a *vir*-dependent pathway; however, transfer of VirE2 and the T-strand–VirD2 complex can occur independently. A *virE2* mutant can transfer T strands into plant cells, and a *virE*$^+$ strain that lacks T-DNA can export VirE2 into plant cells; thus, inoculation of two such nonpathogenic strains onto the same plant wound restores tumorigenesis (41). This phenomenon, called extracellular complementation, requires functional VirB proteins, VirD4, and loci (*chvA*, *chvB*, and *exoC*) necessary for binding of *A. tumefaciens* to plant cells (10). The latter observation indicates that the *virE*$^+$ strain probably exports VirE2 directly into plant cells, rather than into the *virE2* mutant.

Additional evidence shows that VirE2 and T strands can be exported separately to plant cells. First, export of VirE2, but

* Corresponding author. Phone: (541) 737-1791. Fax: (541) 737-0497. E-mail: reamw@bcc.orst.edu.

† Oregon State University Agricultural Experiment Station paper 11,085.

‡ Present address: Department of Microbiology, University of Minnesota, Minneapolis, MN 55455.

not of T strands, requires VirE1 (60). Second, mobilization of the IncQ plasmid RSF1010 from *A. tumefaciens* into plant cells through the VirB pore (6, 7) interferes with T-DNA transmission and abolishes tumorigenesis (69) by preventing transfer of VirE2 into plant cells (4). The presence of RSF1010 in *A. tumefaciens* reduces but does not eliminate transfer of T-DNA to plant cells (4). Thus, transfer of T strands can occur even though export of VirE2 is blocked (4, 60).

VirE2, which binds to ssDNA cooperatively (10, 11, 13, 17, 24, 50), plays an important role inside plant cells but not inside *A. tumefaciens*. T strands accumulate to the wild-type level in *virE2* mutants (58, 65), indicating that VirE2 does not stabilize T strands inside bacterial cells. In addition, *virE2* mutants can transfer T strands into plant cells (78), although at an unknown efficiency, proving that VirE2 is not essential for export of T strands. Transgenic tobacco plants that produce VirE2 are susceptible to transformation by *virE* mutant *A. tumefaciens* (14), indicating that VirE2 is necessary inside plant cells.

VirE2 and VirD2 both contain plant nuclear localization signals (NLSs) (14, 26, 30, 52, 61); inside plant cells these signals appear to target both proteins and the T-DNA to the nucleus (48, 62, 80), where the T-DNA integrates into the plant genome. The NLSs in VirD2 and VirE2 are similar to the type found in nucleoplasmin from the amphibian *Xenopus laevis* (47). Proteins are directed to the nucleus by NLS sequences and enter by ATP-dependent active transport through nuclear pores (54). Typical NLSs are short regions rich in basic amino acids (54). Many NLSs, including those in VirE2, VirD2, and nucleoplasmin, are bipartite sequences that contain two interdependent basic domains, both needed for full activity (14, 30, 47). NLS-binding proteins recognize NLSs and direct NLS-containing proteins to nuclear pores, where transport into nuclei occurs (54). The NLS in VirD2 plays an important role in tumorigenesis, presumably by facilitating nuclear entry of the VirD2–T-strand complex (48). However, deletion of this NLS does not abolish tumorigenesis (52), suggesting that VirE2, which contains two bipartite NLSs (14), may also target T strands to plant nuclei. Indeed, purified VirE2 mediates nuclear uptake of fluorescently labeled ssDNA in plant cells (80). A T strand 15 kb long can bind 500 molecules of VirE2 (11) but only one of VirD2; therefore, it seems likely that the VirE2 NLSs play an important role in nuclear transport of T strands.

Here we report the stability, virulence, and ssDNA binding properties of nine mutant VirE2 proteins. A deletion removed 10 amino acids from a serine-rich putative protein-protein interaction motif but had little effect on tumorigenesis or ssDNA binding. Eight mutations were insertions of *Xho*I linker oligonucleotides throughout *virE2*. Two of the insertions in the C-terminal half of VirE2 destroyed its ability to bind ssDNA. Other insertions, located in the N-terminal half of VirE2, affected the cooperativity of ssDNA binding: one mutation reduced cooperativity whereas another dramatically increased cooperativity. One particularly interesting insertion in the central portion of *virE2* did not affect ssDNA binding but profoundly reduced tumorigenesis. This mutation may interfere with export of VirE2 into plant cells or import into nuclei; alternatively, this mutation may disrupt an uncharacterized activity of VirE2 that is crucial for tumorigenesis.

MATERIALS AND METHODS

Bacterial strains. Table 1 lists the bacterial strains and plasmids used. All strains of *A. tumefaciens* were derived from A348, which harbors the octopine-type Ti plasmid pTiA6NC in the C58 chromosomal background (23).

Media and bacteriological methods. Drug-resistant bacteria were selected on ampicillin (50 μg/ml) and tetracycline (10 μg/ml) in L agar or broth for *Escherichia coli* (38) and carbenicillin (100 μg/ml), kanamycin (100 μg/ml), and gentamicin (50 μg/ml) in AB-glucose agar or YEP (yeast extract-peptone) broth (23) for *A. tumefaciens*. Plasmid DNA was transformed into *E. coli* by the rubidium chloride or calcium chloride method (38); the freeze-thaw method was used for *A. tumefaciens* (27).

A *virE2* null strain. To create a null allele, we replaced 1,496 bp of the *virE2* coding region with the kanamycin resistance gene (*nptII*) from Tn5 (33). The *virE* operon of pTiA6NC lies within a 3.2-kb *Xho*I restriction fragment, which we inserted into the *Sal*I site of pUC18 (75); *lacZ* and the *virE* operon are transcribed in the same direction in the resulting plasmid, pGR1 (60). *virE2* has a single *Stu*I site 30 bp from the 5′ end and *Nae*I sites 835 and 76 bp from the 3′ end (74). We digested pGR1 with *Stu*I and *Nae*I and purified the remainder of pGR1 by agarose gel electrophoresis, thereby removing 1,497 bp of the *virE2* coding sequence. To the blunt-ended *Stu*I- and *Nae*I-cut pGR1 fragment, we ligated a 2.4-kb blunt-ended *Hin*cII restriction fragment that contains the *nptII* gene from Tn5. This created a selectable null allele, *virE2::nptII-1* (Fig. 1). The resulting plasmid, pPD15, contains a single *Bam*HI site which we used to insert pPD15 into the *Bam*HI site of broad-host-range plasmid pRK310 (19) to form pPD16. We transformed pPD16 into A348 and used a marker exchange procedure (23, 49) to isolate a homogenote (WR5000) carrying the kanamycin resistance *virE2::nptII-1* allele in the Ti plasmid. The structure of the Ti plasmid in WR5000 was verified by Southern blot analysis (38) (data not shown).

Mutagenesis of *virE2*. We performed linker insertion mutagenesis on pGR1, which contains the entire *virE* operon, to create mutations throughout *virE2*. Each insertion coded for two additional amino acids without changing the reading frame or adding a stop codon. First, pGR1 was cut once with one of the following restriction endonucleases, which produce blunt ends: *Nae*I, *Pvu*II, *Rsa*I, *Stu*I, and *Xmn*I. Ethidium bromide (0.02 mg/ml) was added to digestion mixtures with restriction enzymes having multiple targets in pGR1 to maximize the amount of pGR1 DNA that was cut only once. Full-length linear DNA (1 μg) was purified by agarose gel electrophoresis, mixed with 1.7 μg of phosphorylated *Xho*I linker oligonucleotide (5′-CTCGAGCTCGAG-3′) and 4 U of T4 DNA ligase (Bethesda Research Laboratories), and incubated overnight at 15°C. After ligation, the DNA was precipitated in ethanol, redissolved in restriction buffer, digested with *Xho*I, and subjected to electrophoresis through a 1% low-melting-temperature agarose gel (SeaPlaque; FMC Bioproducts) cast in TAE (0.04 M Tris-acetate [pH 8], 0.002 M EDTA). We excised linear plasmid DNA, melted the agarose at 70°C, and added 4 μl of ligation buffer (Bethesda Research Laboratories), 6.5 μl of water, and 1.5 U of T4 DNA ligase to 10 μl of the molten DNA-containing agarose. The ligation mixture was incubated overnight at room temperature and then heated to 70°C prior to transformation into *E. coli* MM294 or DH5α. Insertions were mapped with *Xho*I and *Bam*HI, which cuts once in the multiple-cloning site of pGR1, approximately 700 bp upstream from the start of *virE1*; *Xho*I cuts only at the site of the mutation. We sequenced each mutation with an Applied Biosystems model 373 sequencer using the dye-terminator method to show that other alterations did not occur during linker insertion. This mutagenesis yielded eight mutant derivatives of pGR1, pPD1 to pPD8 (Table 1). Figure 2 shows the location of each insertion and the identities of the codons inserted. One insertion, *virE2-472*, also changed the codon preceding the insertion (codon 472) from one encoding a tyrosine to one encoding a serine.

Codons 56 through 65 were deleted from *virE2* by performing oligonucleotide-directed mutagenesis (35) on pPD20 (Table 1). This produced pPD25 (Table 1), from which we excised a 536-bp *Stu*I-*Bgl*II restriction fragment containing the mutation *virE2-1* (Fig. 2); we confirmed the sequence of the entire restriction fragment. We inserted this mutant fragment into pGR1 in place of the wild-type counterpart, creating pPD10 (Table 1).

Virulence assays. The mutant derivatives of pGR1, pPD1 through pPD10, (Table 1) were cut at their single *Bam*HI site and inserted into the *Bam*HI site of broad-host-range plasmid pRK310 such that the *virE* operon and the *lacZ* gene of pRK310 were transcribed in the same direction. This resulted in plasmids pPD101 through pPD110 (Table 1). These plasmids were introduced into the *virE2* null strain WR5000. For quantitative tumorigenesis assays, we infected potato tuber disks (7-mm diameter) as described previously (53). *A. tumefaciens* was grown overnight at 28°C with aeration in YEP broth containing the appropriate antibiotics, harvested by centrifugation, and suspended in phosphate-buffered saline (3 mM monobasic potassium phosphate, 10 mM dibasic sodium phosphate, 120 mM sodium chloride; pH 7.2) (45). Each disk was inoculated with 10 μl (approximately 1×10^7 to 2×10^7 CFU) of *A. tumefaciens*. Carrot slices were inoculated similarly. Leaves of *Kalanchoe daigremontiana* and stems of tomato (cv. Bonnie Best) were infected by wounding them with a sterile toothpick and packing wounds with *A. tumefaciens* cultured on AB-glucose agar containing appropriate antibiotics. The potato disks and carrot slices were scored after 3 weeks, and inoculated leaves and stems were scored after 4 weeks.

Fusion of *virE* to an *E. coli* promoter. We fused the *virE* operon to the *trc* promoter in a derivative of pTrc99A (2) (Pharmacia) to produce VirE1 and VirE2 in *E. coli*. First, we eliminated the *Sph*I restriction site that lies outside the multiple-cloning region of pTrc99A. Following a limited digestion of pTrc99A with *Sph*I, we isolated full-length linear plasmid DNA molecules by agarose gel electrophoresis and created blunt ends by incubation with T4 DNA polymerase and deoxynucleoside triphosphates. The blunt-ended molecules were ligated into circular molecules and transformed into *E. coli*. From among these transformants, we isolated pBL17, a derivative of pTrc99A with a single *Sph*I site that lies in the multiple-cloning region. We cleaved pBL17 with *Nco*I and *Sph*I and ligated to it an annealed pair of DNA oligonucleotides with *Nco*I and *Sph*I

TABLE 1. Bacterial strains and plasmids used in this study

Strain or plasmid	Characteristics	Reference
Strains		
E. coli		
DH5α	F⁻ *recA1 gyrA96 thi-1 hsdR17 supE44 relA1 deoR* Δ*(lacZYA-argF)U196* ϕ80*dlacZ*Δ*M15*	3
CJ236	*dut-1 ung-1 thi-1 relA1* (pCJ105); chloramphenicol resistant	35
JC10,289	F⁻ Δ*(srl-recA)306*::Tn*10 thr-1 leuB6 thi-1 lacY1 galK2 ara-14 xyl-5 proA2 his-4 argE3 rspL31 tsx-33 supE44 mtl-1*	16
MM294	F⁻ *endA1 thi-1 hsdR17 supE44*	49
A. tumefaciens		
A348	pTiA6NC in C58 chromosomal background	23
WR5000	pTiA6NC with *virE2* replaced by *nptII*	This work
WR5100	pPD100 in WR5000	This work
WR5101 to WR5108	pPD101 to pPD108 in WR5000	This work
WR5110	pPD110 in WR5000	This work
Plasmids		
pBL17	pTrc99A with a single *Sph*I site	This work
pGR1	*virE* operon on 3.2-kb *Xho*I fragment in pUC18 *Sal*I site	60
pPD1 to pPD8	pGR1 with *Xho*I linker 30, 281, 638, 768, 1,133, 1,414, 1,489, or 1,526 bp, respectively, from *virE2* start	This work
pPD10	pGR1 with codons 56 to 65 of *virE2* deleted	This work
pPD15	pGR1 with *virE2* replaced by *nptII*	This work
pPD16	pPD15 in *Bam*HI site of pRK310	This work
pPD20	pUC118 with 1.9-kb *Eco*RI fragment of *virE2* (5′ end)	This work
pPD25	pPD20 with codons 56 to 65 of *virE2* deleted	This work
pPD100	pGR1 in *Bam*HI site of pRK310	This work
pPD101 to pPD108	pPD1 to pPD8 in *Bam*HI site of pRK310	This work
pPD110	pPD10 in *Bam*HI site of pRK310	This work
pPD201 to pPD208	pWR223 with *virE2* mutant *Sph*I fragments from pPD1 to pPD8	This work
pPD210	pWR223 with *Sph*I fragment containing *virE2-1* from pPD10	This work
pRK310	IncPα broad-host-range plasmid; *tetA*; pUC9 cloning site	19
pTrc99A	*trc* promoter; *lacI*^{q}	2
pWR223	pBL17 with first 7 codons of *virE1* as *Nco*I-*Sph*I fragment	This work
pWR225	pWR223 with wild-type *virE* operon (from pGR1)	This work

cohesive ends (Fig. 3) to create pWR223 (Table 1). The annealed oligonucleotides contained the first seven codons of *virE1*; the first codon (ATG) occupied the *Nco*I-compatible end, and the sequence contained the only *Sph*I site in the *virE* operon. Plasmid pGR1 contains two *Sph*I sites, one in *virE1* and another in the multiple-cloning region of the pUC18 moiety, beyond the 3′ end of *virE2*. By inserting the *Sph*I fragment into pWR223 (in the proper orientation), we reconstructed the *virE* operon downstream from a strong, lactose-inducible promoter, thereby creating pWR225 (Table 1). Plasmids that contain mutant *virE2* genes were made the same way and transformed into *E. coli* JC10,289, a *recA* mutant (Table 1).

Extract preparation. Twenty-milliliter cultures of *E. coli* harboring wild-type or mutant *virE2* in pBL17 were grown at 37°C in L broth with aeration to an optical density at 595 nm of 0.7. The *trc* promoter was induced by the addition of isopropyl-β-D-thiogalactopyranoside (IPTG) (0.5 mM), and the incubation was continued for 3 h. Cells were harvested by centrifugation (9,500 rpm, Sorvall SS34 rotor, 4°C), resuspended in 1.5 ml of buffer A (10 mM Tris-HCl [pH 8], 10% glycerol, 25 mM sodium chloride, 1 mM phenylmethylsulfonyl fluoride [PMSF], 1 mM dithiothreitol), and lysed in a French press. The lysates were subjected to centrifugation (12,000 rpm, SS34 rotor, 4°C), and 50-μl volumes of the supernatants were frozen at −80°C. The protein concentration in each extract was determined by the Bradford dye-binding procedure (5).

Immunoblot analysis. The amount of VirE2 in each extract was estimated by standard immunoblot methods (3). Known amounts of purified VirE2, together with several different volumes of extracts containing VirE2, were subjected to electrophoresis on a sodium dodecyl sulfate-polyacrylamide gel. Proteins were electrophoretically transferred from the gel to a nitrocellulose membrane, and the membrane was incubated for 30 min at 20°C in MTBS (20 mM Tris-HCl [pH 7.5], 500 mM sodium chloride, 5% [wt/vol] Carnation nonfat dry milk). MTBS was replaced with TTBS (20 mM Tris-HCl [pH 7.5], 500 mM sodium chloride, 0.1% Tween 20) containing a 1:4,000 dilution of polyclonal rabbit antiserum raised against VirE2 (17), and the incubation was continued for 45 min. Prior to use, the antiserum was incubated in TTBS at 37°C for 30 min with a 1:80 dilution of *E. coli* protein extract (Promega). After incubation with the anti-VirE2 antiserum, the membrane was washed twice, for 5 min each, with TTBS. Next, the membrane was incubated for 45 min with a 1:5,000 dilution of goat anti-rabbit antiserum conjugated to horseradish peroxidase (Bio-Rad); this incubation was performed at 20°C in MTTBS (TTBS containing 5% [wt/vol] Carnation nonfat dry milk). The antiserum was removed, and the membrane was washed twice with TTBS (5 min each) and then twice with TBS (TTBS minus Tween 20; 10 min each). The horseradish peroxidase was detected with an ECL Western blot chemiluminescence development kit (Amersham). To quantitate light emissions, we exposed the filters to flashed X-ray film and measured the band intensity with a Molecular Dynamics densitometer coupled to ImageQuant software. For each immunoblot, we used purified VirE2 to establish a linear relationship between the band intensity and the amount of VirE2 in each lane; this standard curve allowed us to determine the amount of VirE2 in each extract.

DNA binding assays. We assessed the ssDNA binding activity of each mutant VirE2 protein. A 517-bp *Hin*fI fragment from pUC18 was labeled with DNA polymerase I (Klenow fragment) and [α-^{32}P]dATP (38); the labeled DNA was made single stranded by boiling. Protein extracts containing VirE2 were mixed with 1 ng of ^{32}P-labeled ssDNA (10-μl total volume) and incubated for 10 min on ice. Loading solution (3 μl of 10% glycerol–0.1% bromphenol blue) was

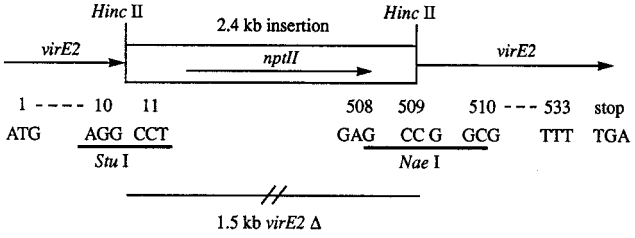

FIG. 1. Replacement of *virE2* with *nptII*. Numbers indicate codons in the wild-type *virE2* gene. Arrows indicate the direction of transcription. Restriction sites used in the construction of pPD15 are indicated.

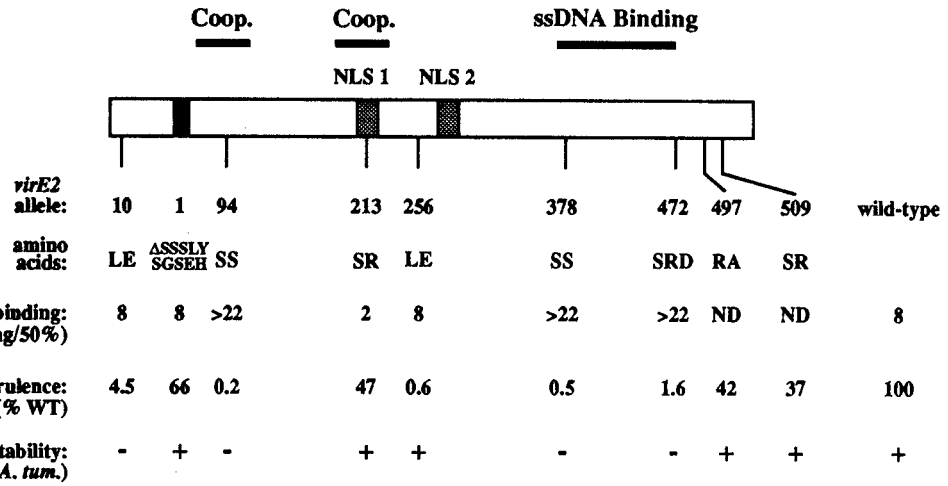

FIG. 2. Mutations in *virE2*. Allele numbers 10 through 509 indicate the codon immediately preceding each *Xho*I linker insertion; the deletion of codons 56 to 65 is indicated by the black box. Amino acids inserted (or removed in the case of *virE2-1*) are indicated in the standard single-letter code. Binding values are the amounts (in nanograms) of wild-type or mutant VirE2 needed to bind 50% of the ssDNA probe. Virulence values are 100 times the mean number of tumors per potato disk induced by a mutant strain divided by the mean tumors/disk induced by WR5100 (WT) (Table 2). "Stability" refers to whether mutant VirE2 accumulates to normal (+) or subnormal (−) levels in acetosyringone-induced *A. tumefaciens*. Bars above the map indicate regions required for binding to ssDNA or for cooperative (Coop.) binding. The shaded boxes represent NLSs; NLS1 occupies codons 205 to 221 (KLRPEDRYVQTERYGRR), and NLS2 includes codons 273 to 287 (KRRYGGET EIKLKSK). ND, not determined.

added prior to electrophoresis on a 4% polyacrylamide gel cast in low-ionic-strength buffer (6.7 mM Tris-HCl [pH 7.5], 1 mM EDTA, 3.3 mM sodium acetate). A potential of 75 V was applied to the gel for 15 min at 4°C prior to loading samples and for 1 h 15 min after loading. The gel was dried and exposed to a PhosphorImager screen. Signals were quantitated with a Molecular Dynamics PhosphorImager with ImageQuant software. The signal which shifted to the top of the gel due to binding to VirE2 was divided by the total signal in each lane; this took into account small differences in the amount of labeled ssDNA loaded in each lane. To test for ssDNA binding by other proteins in the extracts, we incubated labeled ssDNA with an extract from *E. coli* containing only pTrc99A; the amount of protein added (estimated by the Bradford dye-binding method) equalled the total protein in incubation mixtures containing the most VirE2. The control extracts shifted only 3 to 6% of the labeled ssDNA probe to the top of the gel, indicating that the contribution by other ssDNA-binding (SSB) proteins was minimal.

RESULTS

Proteolysis of VirE2 in *E. coli*. A fraction of the VirE2 protein produced in *E. coli* was cleaved by an unidentified cellular protease, in spite of the presence of the protease inhibitor phenyl methylsulfonyl fluoride during extract preparation; cleavage of VirE2 may have occurred during cell growth. Therefore, the VirE2 antiserum recognized two species: full-length VirE2, which exhibited the same electrophoretic mobility as a 66,000-molecular-weight standard (bovine serum albumin), and a slightly smaller species (apparent molecular weight, ~64,000) that migrated as a separate band during sodium dodecyl sulfate-polyacrylamide gel electrophoresis. The signal from both bands was used to estimate the amount of VirE2. In most preparations, approximately half of the VirE2 protein appeared to be full length (data not shown). However, cells harboring insertions *virE2-497* and *virE2-509* contained mostly the smaller form of VirE2, whereas insertion *virE2-94* rendered VirE2 resistant to this proteolysis (data not shown). Due to the increased cleavage of VirE2, we were unable to determine the effects of the *virE2-497* and *virE2-509* mutations on ssDNA binding.

Abolition of DNA binding and virulence. Insertion mutations *virE2-378* and *virE2-472*, which lie in the 3′ half of *virE2* (Fig. 2), severely reduced tumorigenesis (Table 2; Fig. 4) and eliminated binding to ssDNA (Fig. 5e). *A. tumefaciens* strains carrying these insertions had avirulent phenotypes similar to that of WR5000, a *virE2* null mutant, when inoculated onto carrot or *K. daigremontiana*, although all three strains occasionally induced tiny tumors on tomato stems (data not shown). Although WR5000 did not form tumors on potato, the *virE2-378* and *virE2-472* mutants induced tumors on potato at an extremely low frequency (Table 2). The *virE2-378* mutation slightly decreased accumulation of VirE2 in *A. tumefaciens*, whereas VirE2 was barely detectable in the *virE2-472* mutant (Fig. 6b).

Changes in cooperativity. Insertions *virE2-94* and *virE2-213*, located in the 5′ half of *virE2* (Fig. 2), influenced the cooperative binding of VirE2 to ssDNA. Highly cooperative DNA binding is characterized by a sigmoidal binding curve (Fig. 7), which results from an abrupt transition from unbound to fully bound ssDNA as the concentration of SSB protein (VirE2)

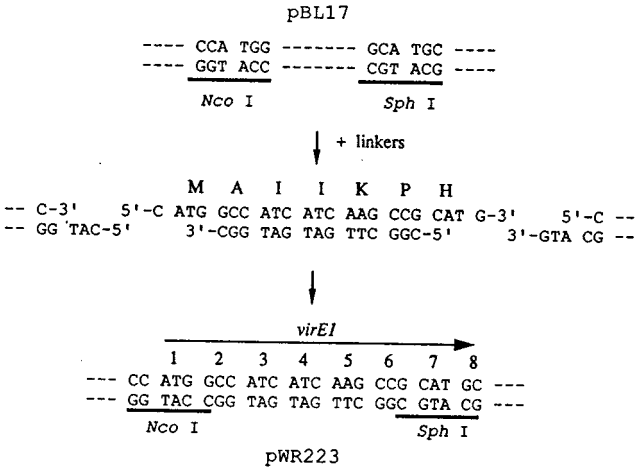

FIG. 3. Construction of pWR223. Annealed oligonucleotides containing the first seven codons of *virE1* were ligated to pBL17 to facilitate expression of the *virE* operon in *E. coli*. Letters indicate the amino acid specified by each codon, numbers are the codon number in *virE1*, and the horizontal arrow indicates the direction of transcription.

TABLE 2. Virulence of *virE2* mutant *A. tumefaciens* on potato

Strain	*virE2* allele	No. of disks	Mean no. of tumors/disk ± SD	Relative virulence[a]
WR5100	Wild type	548	8.3 ± 8.8	100
WR5000	*virE2::nptII-1*	60	0	0
WR5101	*virE2-10*	125	0.37 ± 0.7	4.5
WR5102	*virE2-94*	123	0.02 ± 0.15	0.24
WR5103	*virE2-213*	174	3.9 ± 4.8	47
WR5104	*virE2-256*	273	0.05 ± 0.3	0.60
WR5105	*virE2-378*	79	0.04 ± 0.19	0.48
WR5106	*virE2-472*	88	0.13 ± 0.47	1.6
WR5107	*virE2-497*	133	3.5 ± 4.7	42
WR5108	*virE2-509*	140	3.1 ± 4.7	37
WR5110	*virE2-1*	300	5.5 ± 6.7	66

[a] The relative virulence of each strain is expressed as a percentage of that of WR5100. We used a Student *t* test to determine the probability that the virulence of a *virE2* mutant differed significantly from that of WR5100. A *P* value less than or equal to 0.01 indicates that the two strains almost certainly differ significantly. The virulence of each mutant strain in this table was significantly different from the virulence of WR5100 ($P < 0.01$).

increases over a narrow range. As binding cooperativity decreases, the transition from unbound to fully bound ssDNA occurs over a broader range of SSB concentrations. The *virE2-94* mutation decreased the ability of VirE2 to bind ssDNA cooperatively. Although 10 ng of wild-type VirE2 fully retarded the electrophoretic mobility of all of the labeled ssDNA probe (Fig. 5a), even as much as 22 ng of *virE2-94* mutant VirE2 did not retard migration of the probe fully (Fig. 5b), indicating that the majority of the ssDNA molecules were not completely coated with VirE2. The ssDNA binding curve indicates that this mutation reduced binding cooperativity (Fig. 7). The *virE2-94* allele greatly reduced the accumulation of mutant VirE2 in *A. tumefaciens* (Fig. 6a) and nearly abolished tumorigenesis on all plants tested (Table 2; Fig. 4). Instability of the mutant protein in *A. tumefaciens* probably caused this severe decrease in tumorigenesis.

The insertion *virE2-213* lies in one of the NLSs (NLS1) of VirE2 (Fig. 2). Although deletion of NLS1 decreases ssDNA binding cooperativity (14), the *virE2-213* mutation increased cooperative ssDNA binding (Fig. 5c). This resulted in a sharp transition from unbound to fully bound ssDNA probe that occurred over a very narrow range of VirE2 concentrations (0 to 2.2 ng) (Fig. 5c and 7). The *virE2-213* mutation slightly decreased tumorigenesis on potato disks, to 47% of the wild-type level (Table 2; Fig. 4). A Student *t* test (36) indicated that this modest difference was significant ($P < 0.01$); however, this strain appeared to be fully virulent on *K. daigremontiana*, carrot, and tomato (data not shown). This insertion did not affect the accumulation of mutant VirE2 in *A. tumefaciens* (Fig. 6a).

Wild-type ssDNA binding and virulence. VirE2 shares a serine-rich region (SSSLYSGSEH) with another SSB, phage T4 gene 32 protein (gp32) (SSSGSSSS). Because this region of gp32 interacts with other proteins during T4 DNA replication (31, 34), we tested the importance of this serine-rich motif in VirE2. Deletion of these 10 amino acids near the N terminus of VirE2 (*virE2-1* [Fig. 2]) had little effect on the ability of VirE2 to bind ssDNA (Fig. 5e and 7) or on tumorigenesis (Table 2; Fig. 4). *A. tumefaciens* containing mutation *virE2-1* was fully virulent on carrot, *K. daigremontiana*, and tomato (data not shown), and the mutant protein was stable in *A. tumefaciens* (Fig. 6c). Consequently, this serine-rich region was not important for VirE2 function.

Wild-type ssDNA binding and decreased virulence. Insertions *virE2-10* (near the 5′ end of *virE2*) and *virE2-256* (in the center of *virE2*) significantly reduced tumorigenesis on potato disks (Table 2; Fig. 4) without affecting the ability of these mutant VirE2 proteins to bind ssDNA (Fig. 5 and 7). The *virE2-10* mutation severely decreased tumorigenesis on potato disks (4.5% of the wild type [Table 2; Fig. 4]) and carrot (data not shown). *A. tumefaciens* containing mutation *virE2-10* was tumorigenic on tomato and exhibited variable virulence on *K. daigremontiana*, forming small to normal-sized tumors (data not shown). The *virE2-10* allele destabilized mutant VirE2 in *A. tumefaciens* (Fig. 6a), which probably accounts for the reduction in tumorigenesis resulting from this mutation.

Insertion *virE2-256* did not diminish the ability of mutant VirE2 to bind ssDNA (Fig. 5d and 7); however, this mutation drastically reduced tumorigenesis on carrot (Fig. 8) and on potato disks (0.6% of the wild type [Table 2; Fig. 4 and 8]). Fewer tumors appeared on tomato and smaller tumors formed on *K. daigremontiana* inoculated with the *virE2-256* mutant than on plants inoculated with wild-type *A. tumefaciens* (data not shown). The mutant VirE2 protein produced by the *virE2-256* strain was stable in *A. tumefaciens* (Fig. 6a). This mutation must affect an important property of VirE2 other than its ssDNA binding activity; for example, the *virE2-256* allele may interfere with VirE1-dependent export into plant cells or nuclear localization.

Insertions near the C terminus. Linker insertion mutations *virE2-497* and *virE2-509* destabilized the corresponding mutant VirE2 proteins in *E. coli* (data not shown), which prevented an accurate determination of the ssDNA binding abilities of these proteins. Both mutations affect VirE2 near the C terminus (Fig. 2), and each insertion reduced tumorigenesis on potato disks to about 40% of the wild-type level (Table 2; Fig. 4). Tumorigenesis was also reduced on carrot, but both mutants exhibited full virulence on *K. daigremontiana* and tomato (data not shown). Each of these mutant VirE2 proteins accumulated

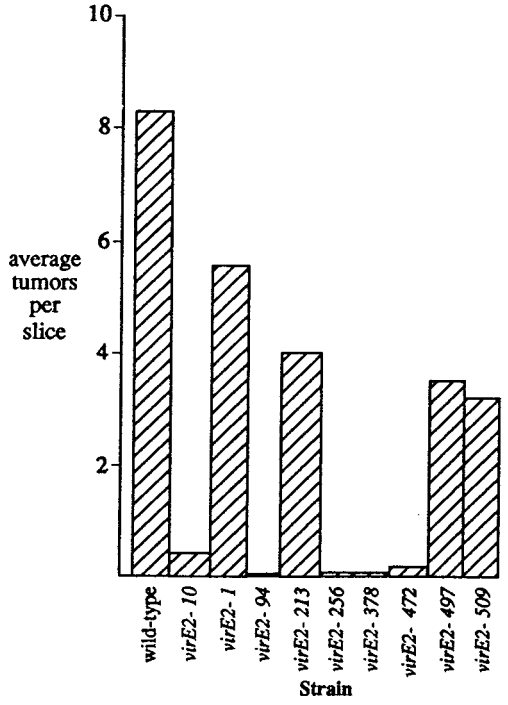

FIG. 4. Virulence of *virE2*-mutant *A. tumefaciens* on potato. The data contained in Table 2 are summarized in graph form; shown are the mean numbers of tumors/disk that arose on potato 3 weeks after inoculation.

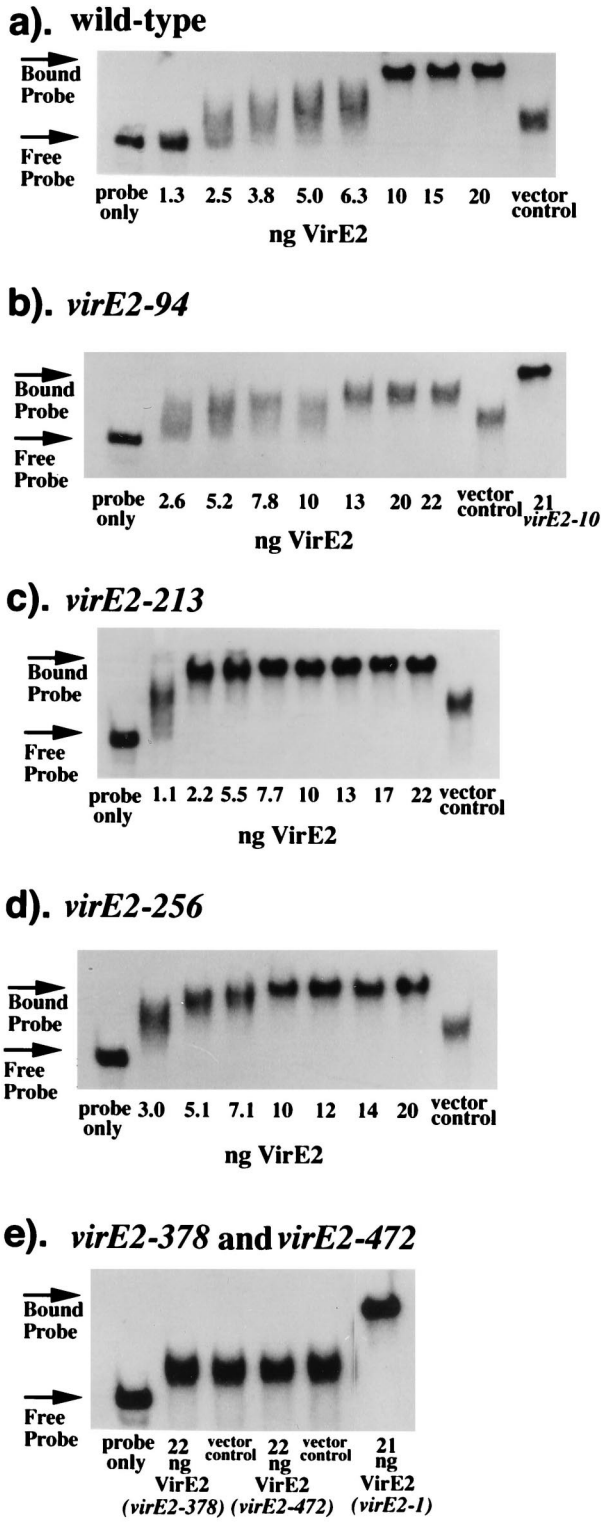

FIG. 5. ssDNA binding by mutant VirE2. Extracts from *E. coli* that produce VirE1 and wild-type or mutant VirE2 were assayed for ssDNA binding activity. Lanes marked "vector control" contain proteins extracted from *E. coli* that harbor pTrc99A (without the *virE* operon); the amount of protein added equalled the total protein in incubation mixtures containing 22 ng of VirE2. (a) Wild-type VirE2; (b) mutant VirE2 showing reduced cooperativity (*virE2-94* allele); (c) mutant VirE2 showing increased cooperativity (*virE2-213* allele); (d) mutant VirE2 showing wild-type ssDNA binding (weakly pathogenic *virE2-256* allele); (e) mutant VirE2 proteins that do not bind ssDNA (*virE2-378* and *virE2-472* alleles). Mutant VirE2 proteins that exhibited wild-type ssDNA binding were included for panels b (*virE2-10* allele) and e (*virE2-1* allele).

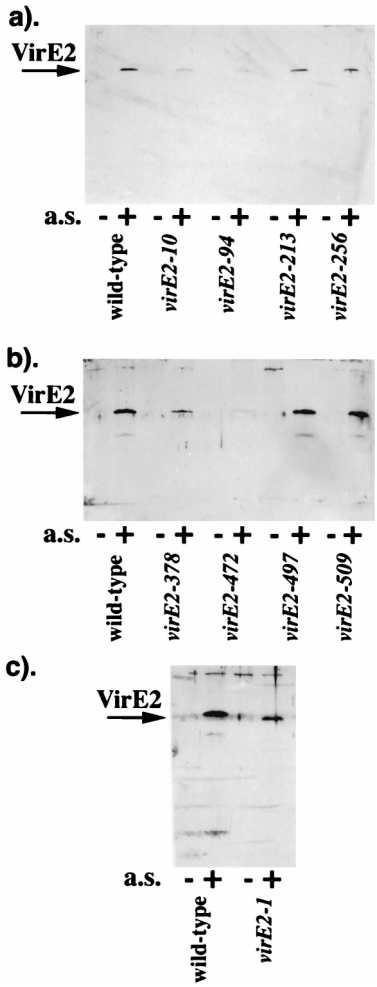

FIG. 6. Accumulation of mutant VirE2 in *A. tumefaciens*. Immunoblots of proteins extracted from *A. tumefaciens* cultured in the presence (+) or absence (−) of acetosyringone (a.s.) indicate the level of VirE2 contained in each mutant strain. Arrows indicate the electrophoretic mobility of purified wild-type VirE2. Allele numbers indicate which mutant *virE2* gene encoded the VirE2 protein contained in each lane.

to the wild-type level in *A. tumefaciens* (Fig. 6b). Because both mutations had only a modest effect on tumorigenesis, we infer that these mutations did not decrease significantly the ability of the mutant proteins to bind ssDNA.

DISCUSSION

The C-terminal half of VirE2 is required for ssDNA binding, but the N-terminal half appears to be nonessential for SSB activity. Two mutations in the C-terminal region, *virE2-378* and *virE2-472*, eliminated ssDNA binding, whereas mutations that altered the N-terminal half of VirE2 did not abolish ssDNA binding. Deletion of NLS2, which lies near the center of VirE2, abolishes ssDNA binding (14), and ssDNA binding is also eliminated if both the C-terminal lysine residues of NLS2 are replaced with glycine residues (12). In addition, elimination of 36 C-terminal residues from VirE2 destroys its ability to bind ssDNA (17). The work reported here confirms that the region of VirE2 from NLS2 to the C terminus is essential for binding to ssDNA, and this study establishes that the N-terminal region is not required for ssDNA binding.

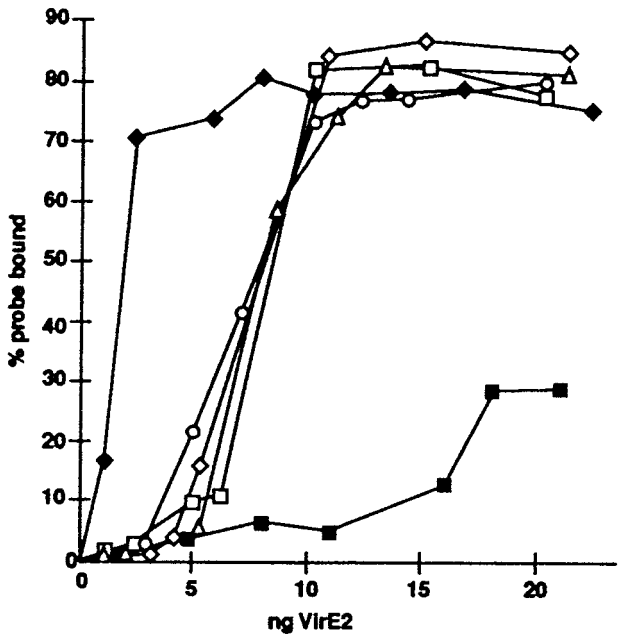

FIG. 7. ssDNA binding by wild-type and mutant VirE2. The symbols indicate VirE2 encoded by *virE2* alleles, as follows: □, wild type; △, *virE2-1*; ◇, *virE2-10*; ■, *virE2-94*; ◆, *virE2-213*; and ○, *virE2-256*.

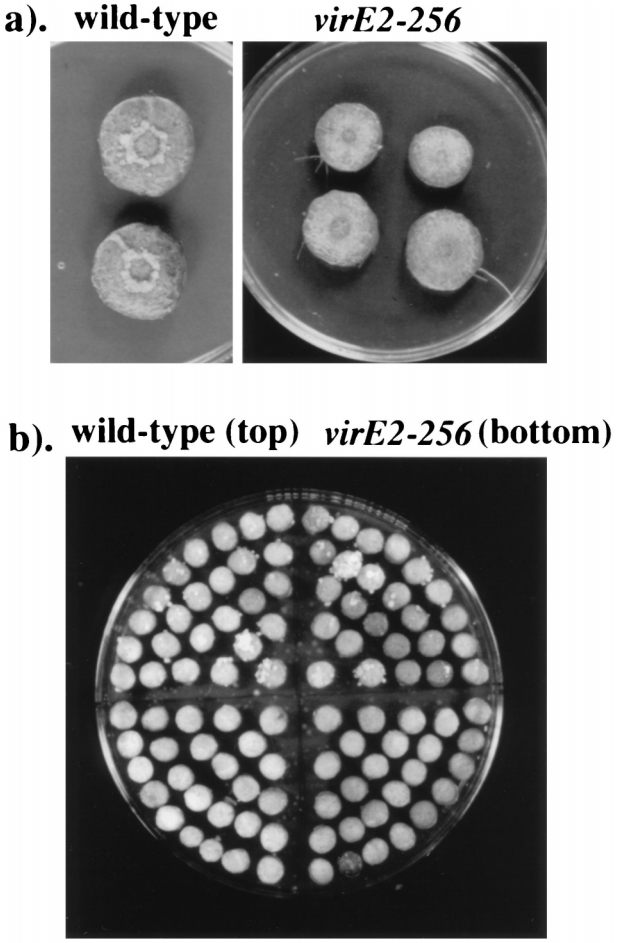

FIG. 8. Virulence of WR5100 (*virE2*$^+$) and WR5104 (*virE2-256*) on carrot (a) and potato (b).

The *virE2-94* and *virE2-213* insertions define regions that influence the cooperativity of ssDNA binding. The *virE2-94* mutation decreased cooperativity and also rendered the mutant VirE2 protein unstable in *A. tumefaciens*. This instability likely accounts for the large decrease in virulence caused by this mutation. *virE2-94* provided the first evidence that the region near the N terminus of VirE2 is involved in cooperative ssDNA binding. Deletion of NLS1, which lies near the center of VirE2, reduces the cooperativity of ssDNA binding (14). The *virE2-213* mutation, which lies within NLS1, increased the cooperativity of ssDNA binding by mutant VirE2, confirming the importance of this region for cooperative ssDNA binding. The *virE2-213* mutation did not reduce the stability of VirE2 and reduced tumorigenesis only slightly. This decrease in virulence may be due to disruption of one of the two NLSs in VirE2. To determine whether tumorigenesis depends upon cooperative ssDNA binding by VirE2, we must create mutations that eliminate cooperativity without destabilizing the protein or affecting NLS activity. Nevertheless, the *virE2-213* mutation, which increased cooperativity, should prove useful in future studies of protein-protein interactions involved in cooperative ssDNA binding.

Two mutations, *virE2-10* and *virE2-256*, reduced tumorigenesis but had no effect on ssDNA binding. Immunoblots showed that the *virE2-10* insertion significantly reduced accumulation of VirE2 in *A. tumefaciens*, which probably accounts for the 20-fold decrease in tumorigenesis caused by this mutation. In contrast, the *virE2-256* allele encoded a mutant VirE2 protein that was stable in *A. tumefaciens* and retained wild-type ssDNA binding activity. Therefore, this mutation must alter an important property of VirE2 other than ssDNA binding or protein stability. The *virE2-256* mutation may inhibit an activity of VirE2 inside plant cells. Because the *virE2-256* insertion lies between the two NLSs of VirE2, it may interfere with nuclear localization of VirE2 or VirE2-bound T strands. However, the *virE2-256* mutation instead may affect integration of incoming T-strand DNA into the plant genome, suggesting a role for VirE2 in T-DNA integration, which was proposed previously (21).

Alternatively, the *virE2-256* mutation may block tumorigenesis at an early step by preventing export of VirE2 into plant cells. VirE1 is required for export of VirE2 into plant cells (60), suggesting a direct interaction between VirE1 and VirE2. Additional observations support the idea of direct VirE1-VirE2 contact. Although VirE2 is stable in *A. tumefaciens* without VirE1 (60), VirE1 is required for the stability of VirE2 in *E. coli* (19a, 39). Because extracts from strains harboring either the wild-type or *virE2-256* allele contained similar quantities of active VirE2, it is unlikely that this insertion affects the putative stabilizing interaction between VirE2 and VirE1. Export of VirE2 also depends upon VirD4 and proteins encoded by the *virB* operon (10). The *virE2-256* mutation may prevent an interaction with one or more of these proteins and thereby block export of VirE2 from *A. tumefaciens*. Further experimentation will be needed to establish the reason this mutation decreases crown gall tumorigenesis.

ACKNOWLEDGMENTS

We thank Anath Das for providing antibodies to VirE2, Brian Lanoil for constructing pBL17, and Christopher Sundberg and Larry Hodges for critical reading of this paper.

This work was supported by USDA grant 93-37301-8728.

REFERENCES

1. **Albright, L. M., M. F. Yanofsky, B. Leroux, D. Ma, and E. W. Nester.** 1987. Processing of the T-DNA of *Agrobacterium tumefaciens* generates border nicks and linear, single-stranded T-DNA. J. Bacteriol. **169:**1046–1055.
2. **Amann, E., B. Ochs, and K. J. Abel.** 1988. Tightly regulated *tac* promoter vectors useful for the expression of unfused and fused proteins in *Escherichia coli*. Gene **69:**301–315.
3. **Ausubel, F. M., R. Brent, R. E. Kingston, D. D. Moore, J. G. Seidman, J. A. Smith, and K. Struhl (ed.).** 1987. Current protocols in molecular biology. Wiley, New York, N.Y.
4. **Binns, A. N., C. E. Beaupre, and E. M. Dale.** 1995. Inhibition of VirB-mediated transfer of diverse substrates from *Agrobacterium tumefaciens* by the IncQ plasmid RSF1010. J. Bacteriol. **177:**4890–4899.
5. **Bradford, M. M.** 1976. A rapid and sensitive method for the quantitation of microgram quantities of protein utilizing the principle of protein-dye binding. Anal. Biochem. **72:**248–254.
6. **Buchanan-Wollaston, V., J. E. Passiatore, and F. Cannon.** 1987. The *mob* and *oriT* mobilization functions of a bacterial plasmid promote its transfer to plants. Nature **328:**172–175.
7. **Buchanan-Wollaston, V., J. E. Passiatore, and F. Cannon.** 1988. The effect of *vir* mutations on plasmid transfer into plants, p. 281–282. *In* R. Palachios and D. P. S. Verma (ed.), Molecular genetics of plant-microbe interactions. APS Press, St. Paul, Minn.
8. **Chilton, M. D., M. H. Drummond, D. J. Merlo, D. Sciaky, A. L. Montoya, M. P. Gordon, and E. W. Nester.** 1977. Stable incorporation of plasmid DNA into higher plant cells: the molecular basis of crown gall tumorigenesis. Cell **11:**263–271.
9. **Chilton, M. D., R. K. Saiki, N. Yadav, M. P. Gordon, and F. Quetier.** 1980. T-DNA from *Agrobacterium* Ti plasmid is in the nuclear DNA fraction of crown gall tumor cells. Proc. Natl. Acad. Sci. USA **77:**4060–4064.
10. **Christie, P. J., J. E. Ward, S. C. Winans, and E. W. Nester.** 1988. The *Agrobacterium tumefaciens virE2* gene product is a single-stranded-DNA-binding protein that associates with T-DNA. J. Bacteriol. **170:**2659–2667.
11. **Citovsky, V., G. De Vos, and P. Zambryski.** 1988. Single-stranded DNA binding protein encoded by the *virE* locus of *Agrobacterium tumefaciens*. Science **240:**501–504.
12. **Citovsky, V., D. Warnick, and P. Zambryski.** 1994. Nuclear import of *Agrobacterium* VirD2 and VirE2 proteins in maize and tobacco. Proc. Natl. Acad. Sci. USA **91:**3210–3214.
13. **Citovsky, V., M. L. Wong, and P. Zambryski.** 1989. Cooperative interaction of *Agrobacterium* VirE2 protein with single-stranded DNA: implications for the T-DNA transfer process. Proc. Natl. Acad. Sci. USA **86:**1193–1197.
14. **Citovsky, V., J. Zupan, D. Warnick, and P. Zambryski.** 1992. Nuclear localization of *Agrobacterium* VirE2 protein in plant cells. Science **256:**1802–1805.
15. **Covacci, A., and R. Rappuoli.** 1993. Pertussis toxin export requires accessory genes located downstream from the pertussis toxin operon. Mol. Microbiol. **8:**429–434.
16. **Csonka, L. N., and A. J. Clark.** 1979. Deletions generated by the transposon Tn*10* in the *srl recA* region of the *Escherichia coli* K-12 chromosome. Genetics **93:**321–343.
17. **Das, A.** 1988. *Agrobacterium tumefaciens virE* operon encodes a single-stranded DNA-binding protein. Proc. Natl. Acad. Sci. USA **85:**2909–2913.
18. **DeCleene, M., and J. DeLey.** 1976. The host range of crown gall. Bot. Rev. **42:**389–466.
19. **Ditta, G., T. Schmidhauser, E. Yakobson, P. Lu, X. Liang, D. R. Finlay, D. Guiney, and D. R. Helinski.** 1985. Plasmids related to the broad-host-range vector, pRK290, useful for gene cloning and for monitoring gene expression. Plasmid **13:**149–153.

19a. **Dombek, P., and W. Ream.** Unpublished data.

20. **Durrenberger, F., A. Crameri, B. Hohn, and Z. Koukolikova-Nicola.** 1989. Covalently bound VirD2 protein of *Agrobacterium tumefaciens* protects the T-DNA from exonucleolytic degradation. Proc. Natl. Acad. Sci. USA **86:**9154–9158.
21. **Gardner, R. C., and V. C. Knauf.** 1986. Transfer of *Agrobacterium* DNA to plants requires a T-DNA border but not the *virE* locus. Science **231:**725–727.
22. **Garfinkel, D. J., and E. W. Nester.** 1980. *Agrobacterium tumefaciens* mutants affected in crown gall tumorigenesis and octopine catabolism. J. Bacteriol. **144:**732–743.
23. **Garfinkel, D. J., R. B. Simpson, L. W. Ream, F. F. White, M. P. Gordon, and E. W. Nester.** 1981. Genetic analysis of crown gall: fine structure map of the T-DNA by site-directed mutagenesis. Cell **27:**143–153.
24. **Gietl, C., Z. Koukolikova-Nicola, and B. Hohn.** 1987. Mobilization of T-DNA from *Agrobacterium* to plant cells involves a protein that binds single-stranded DNA. Proc. Natl. Acad. Sci. USA **84:**9006–9010.
25. **Herrera-Estrella, A., Z. Chen, M. Van Montagu, and K. Wang.** 1988. VirD proteins of *Agrobacterium tumefaciens* are required for the formation of a covalent DNA-protein complex at the 5′ terminus of T-strand molecules. EMBO J. **7:**4055–4062.
26. **Herrera-Estrella, A., M. Van Montagu, and K. Wang.** 1990. A bacterial peptide acting as a plant nuclear targeting signal: the amino-terminal portion of *Agrobacterium* VirD2 protein directs a beta-galactosidase fusion protein into tobacco nuclei. Proc. Natl. Acad. Sci. USA **87:**9534–9537.
27. **Holsters, M., D. deWaele, A. Depicker, E. Messens, M. Van Montagu, and J. Schell.** 1978. Transfection and transformation of *Agrobacterium tumefaciens*. Mol. Gen. Genet. **163:**181–187.
28. **Hooykaas, P. J. J., and G. M. Beijersbergen.** 1994. The virulence system of *Agrobacterium tumefaciens*. Annu. Rev. Phytopathol. **32:**157–179.
29. **Howard, E. A., B. A. Winsor, G. De Vos, and P. Zambryski.** 1989. Activation of the T-DNA transfer process in *Agrobacterium* results in the generation of a T-strand-protein complex: tight association of VirD2 with the 5′ ends of T-strands. Proc. Natl. Acad. Sci. USA **86:**4017–4021.
30. **Howard, E. A., J. R. Zupan, V. Citovsky, and P. C. Zambryski.** 1992. The VirD2 protein of *Agrobacterium tumefaciens* contains a C-terminal bipartite nuclear localization signal: implications for nuclear uptake of DNA in plant cells. Cell **68:**109–118.
31. **Hurley, J. M., S. A. Chervitz, T. C. Jarvis, B. S. Singer, and L. Gold.** 1993. Assembly of the bacteriophage T4 replication machine requires the acidic carboxy terminus of gene 32 protein. J. Mol. Biol. **229:**398–418.
32. **Jayaswal, R. K., K. Veluthambi, S. B. Gelvin, and J. L. Slightom.** 1987. Double-stranded cleavage of T-DNA and generation of single-stranded T-DNA molecules in *Escherichia coli* by a *virD*-encoded border-specific endonuclease from *Agrobacterium tumefaciens.* J. Bacteriol. **169:**5035–5045.
33. **Jorgensen, R. A., S. J. Rothstein, and W. S. Reznikoff.** 1979. A restriction enzyme cleavage map of Tn*5* and location of a region encoding neomycin resistance. Mol. Gen. Genet. **177:**65–72.
34. **Krassa, K. B., L. S. Green, and L. Gold.** 1991. Protein-protein interactions with the acidic COOH terminus of the single-stranded DNA-binding protein of the bacteriophage T4. Proc. Natl. Acad. Sci. USA **88:**4010–4014.
35. **Kunkel, T. A., J. D. Roberts, and R. A. Zakour.** 1987. Rapid and efficient site-specific mutagenesis without phenotypic selection. Methods Enzymol. **154:**367–382.
36. **Langley, R.** 1970. Practical statistics, p. 160–165. Dover Publications, New York, N.Y.
37. **Lessl, M., D. Balzer, W. Pansegrau, and E. Lanka.** 1992. Sequence similarities between the RP4 Tra2 and the Ti VirB region strongly support the conjugation model for T-DNA transfer. J. Biol. Chem. **267:**20471–20480.
38. **Maniatis, T., E. F. Fritsch, and J. Sambrook.** 1982. Molecular cloning: a laboratory manual. Cold Spring Harbor Laboratory, Cold Spring Harbor, N.Y.
39. **McBride, K. E., and V. C. Knauf.** 1988. Genetic analysis of the *virE* operon of the *Agrobacterium* Ti plasmid pTiA6. J. Bacteriol. **170:**1430–1437.
40. **Okamoto, S., A. Toyoda-Yamamoto, K. Ito, I. Takebe, and Y. Machida.** 1991. Localization and orientation of the VirD4 protein of *Agrobacterium tumefaciens* in the cell membrane. Mol. Gen. Genet. **228:**24–32.
41. **Otten, L., H. DeGreve, J. Leemans, R. Hain, P. J. J. Hooykaas, and J. Schell.** 1984. Restoration of virulence of *vir* region mutants of *Agrobacterium tumefaciens* strain B653 by coinfection with normal and mutant *Agrobacterium* strains. Mol. Gen. Genet. **175:**159–163.
42. **Peralta, E. G., R. Hellmiss, and W. Ream.** 1986. *overdrive*, a T-DNA transmission enhancer on the *A. tumefaciens* tumour-inducing plasmid. EMBO J. **5:**1137–1142.
43. **Peralta, E. G., and L. W. Ream.** 1985. T-DNA border sequences required for crown gall tumorigenesis. Proc. Natl. Acad. Sci. USA **82:**5112–5116.
44. **Pohlman, R. F., H. D. Genetti, and S. C. Winans.** 1994. Common ancestry between IncN conjugal transfer genes and macromolecular export systems of plant and animal pathogens. Mol. Microbiol. **14:**655–668.
45. **Pueppke, S. C., and U. K. Benny.** 1981. Induction of tumors on *Solanum tuberosum* L. by *Agrobacterium*: quantitative analysis, inhibition by carbohydrates, and virulence of selected strains. Physiol. Plant Pathol. **18:**169–179.
46. **Ream, W.** 1989. *Agrobacterium tumefaciens* and interkingdom genetic exchange. Annu. Rev. Phytopathol. **27:**583–618.
47. **Robbins, J., S. M. Dilworth, R. A. Laskey, and C. Dingwall.** 1991. Two interdependent basic domains in nucleoplasmin nuclear targeting sequence: identification of a class of bipartite nuclear targeting sequence. Cell **64:**615–623.
48. **Rossi, L., B. Hohn, and B. Tinland.** 1996. Integration of complete transferred DNA units is dependent on the activity of virulence E2 protein of *Agrobacterium tumefaciens*. Proc. Natl. Acad. Sci. USA **93:**126–130.
49. **Ruvkun, G. B., and F. M. Ausubel.** 1981. A general method for site-directed mutagenesis in prokaryotes. Nature **289:**85–88.
50. **Sen, P., G. J. Pazour, D. Anderson, and A. Das.** 1989. Cooperative binding of the VirE2 protein to single-stranded DNA. J. Bacteriol. **171:**2573–2580.
51. **Shaw, C. H., M. Watson, and G. Carter.** 1984. The right hand copy of the nopaline Ti plasmid 25 bp repeat is required for tumour formation. Nucleic Acids Res. **12:**6031–6041.
52. **Shurvinton, C. E., L. Hodges, and W. Ream.** 1992. A nuclear localization signal and the C-terminal omega sequence in the *Agrobacterium tumefaciens* VirD2 endonuclease are important for tumor formation. Proc. Natl. Acad. Sci. USA **89:**11837–11841.
53. **Shurvinton, C. E., and W. Ream.** 1991. Stimulation of *Agrobacterium tumefaciens* T-DNA transfer by overdrive depends on a flanking sequence but not on helical position with respect to the border repeat. J. Bacteriol. **173:**5558–5563.
54. **Silver, P. A.** 1991. How proteins enter the nucleus. Cell **64:**489–497.

55. **Stachel, S. E., E. Messens, M. Van Montagu, and P. Zambryski.** 1985. Identification of the signal molecules produced by wounded plant cells that activate T-DNA transfer in *Agrobacterium tumefaciens*. Nature **318:**624–629.
56. **Stachel, S. E., and E. W. Nester.** 1986. The genetic and transcriptional organization of the *vir* region of the A6 Ti plasmid of *Agrobacterium tumefaciens*. EMBO J. **5:**1445–1454.
57. **Stachel, S. E., B. Timmerman, and P. Zambryski.** 1986. Generation of single-stranded T-DNA molecules during the initial stages of T-DNA transfer from *Agrobacterium tumefaciens* to plant cells. Nature **322:**706–712.
58. **Stachel, S. E., B. Timmerman, and P. Zambryski.** 1987. Activation of *Agrobacterium tumefaciens vir* gene expression generates multiple single-stranded T-strand molecules from the pTiA6 T-region: requirement of 5′ *virD* gene products. EMBO J. **6:**857–863.
59. **Stachel, S. E., and P. Zambryski.** 1986. *Agrobacterium tumefaciens* and the susceptible plant cell: a novel adaptation of extracellular recognition and DNA conjugation. Cell **47:**155–157.
60. **Sundberg, C., L. Meek, K. Carroll, A. Das, and W. Ream.** 1996. VirE1 protein mediates export of the single-stranded DNA-binding protein VirE2 from *Agrobacterium tumefaciens* into plant cells. J. Bacteriol. **178:**1207–1212.
61. **Tinland, B., Z. Koukolikova-Nicola, M. N. Hall, and B. Hohn.** 1992. The T-DNA-linked VirD2 protein contains two distinct functional nuclear localization signals. Proc. Natl. Acad. Sci. USA **89:**7442–7446.
62. **Tinland, B., F. Schoumacher, V. Gloeckler, A. Bravo-Angel, and B. Hohn.** 1995. The *Agrobacterium tumefaciens* virulence D2 protein is responsible for precise integration of T-DNA into the plant genome. EMBO J. **14:**3585–3595.
63. **Toro, N., A. Datta, O. A. Carmi, C. Young, R. K. Prusti, and E. W. Nester.** 1989. The *Agrobacterium tumefaciens virC1* gene product binds to overdrive, a T-DNA transfer enhancer. J. Bacteriol. **171:**6845–6849.
64. **Van Larebeke, N., G. Engler, M. Holsters, S. Van den Elsacker, I. Zaenen, R. A. Schilperoort, and J. Schell.** 1974. Large plasmid in *Agrobacterium tumefaciens* essential for crown gall inducing activity. Nature **252:**169–170.
65. **Veluthambi, K., W. Ream, and S. B. Gelvin.** 1988. Virulence genes, borders, and overdrive generate single-stranded T-DNA molecules from the A6 Ti plasmid of *Agrobacterium tumefaciens*. J. Bacteriol. **170:**1523–1532.
66. **Wang, K., L. Herrera-Estrella, M. Van Montagu, and P. Zambryski.** 1984. Right 25 bp terminus sequence of the nopaline T-DNA is essential for and determines direction of DNA transfer from *Agrobacterium* to the plant genome. Cell **38:**455–462.
67. **Wang, K., S. E. Stachel, B. Timmerman, M. Van Montagu, and P. Zambryski.** 1987. Site-specific nick in the T-DNA border sequence as a result of *Agrobacterium vir* gene expression. Science **235:**587–591.
68. **Ward, E. R., and W. M. Barnes.** 1988. VirD2 protein of *Agrobacterium tumefaciens* very tightly linked to the 5′ end of T-strand DNA. Science **242:**927–930.
69. **Ward, J. E., E. M. Dale, and A. N. Binns.** 1991. Activity of the *Agrobacterium* T-DNA transfer machinery is affected by *virB* gene products. Proc. Natl. Acad. Sci. USA **88:**9350–9354.
70. **Watson, B., T. C. Currier, M. P. Gordon, M. D. Chilton, and E. W. Nester.** 1975. Plasmid required for virulence of *Agrobacterium tumefaciens*. J. Bacteriol. **123:**255–264.
71. **Weiss, A. A., F. D. Johnson, and D. L. Burns.** 1993. Molecular characterization of an operon required for pertussis toxin secretion. Proc. Natl. Acad. Sci. USA **90:**2970–2974.
72. **Willmitzer, L., M. Debeuckeleer, M. Lemmers, M. Van Montagu, and J. Schell.** 1980. DNA from Ti plasmid present in nucleus and absent from plastids of crown gall plant cells. Nature **287:**359–361.
73. **Winans, S. C.** 1992. Two-way chemical signaling in *Agrobacterium*-plant interactions. Microbiol. Rev. **56:**12–31.
74. **Winans, S. C., P. Allenza, S. E. Stachel, K. E. McBride, and E. W. Nester.** 1987. Characterization of the *virE* operon of the *Agrobacterium* Ti plasmid pTiA6. Nucleic Acids Res. **15:**825–838.
75. **Yanisch-Perron, C., J. Vieira, and J. Messing.** 1985. Improved M13 phage cloning vectors and host strains: nucleotide sequences of the M13mp18 and pUC19 vectors. Gene **33:**103–119.
76. **Yanofsky, M. F., S. G. Porter, C. Young, L. M. Albright, M. P. Gordon, and E. W. Nester.** 1986. The *virD* operon of *Agrobacterium tumefaciens* encodes a site-specific endonuclease. Cell **47:**471–477.
77. **Young, C., and E. W. Nester.** 1988. Association of the VirD2 protein with the 5′ end of T strands in *Agrobacterium tumefaciens*. J. Bacteriol. **170:**3367–3374.
78. **Yusibov, V. M., T. R. Steck, V. Gupta, and S. B. Gelvin.** 1994. Association of single-stranded transferred DNA from *Agrobacterium tumefaciens* with tobacco cells. Proc. Natl. Acad. Sci. USA **91:**2994–2998.
79. **Zambryski, P. C.** 1992. Chronicles from the *Agrobacterium*-plant cell DNA transfer story. Annu. Rev. Plant Physiol. Plant Mol. Biol. **43:**465–490.
80. **Zupan, J. R., V. Citovsky, and P. Zambryski.** 1996. *Agrobacterium* VirE2 protein mediates nuclear uptake of single-stranded DNA in plant cells. Proc. Natl. Acad. Sci. USA **93:**2392–2397.